

# SPARSE SIGNAL REPRESENTATION FOR COMPLEX-VALUED IMAGING

Sadegh Samadi<sup>1</sup>, M üjdat Çetin<sup>2</sup>, Mohammad Ali Masnadi-Shirazi<sup>1</sup>

1. Shiraz University, Shiraz, Iran , 2. Sabanci University, İstanbul, Turkey  
[ssamadi@shirazu.ac.ir](mailto:ssamadi@shirazu.ac.ir) , [mcetin@sabanciuniv.edu](mailto:mcetin@sabanciuniv.edu) , [masnadi@shirazu.ac.ir](mailto:masnadi@shirazu.ac.ir)

**Abstract:** We propose a sparse signal representation-based method for complex-valued imaging. Many coherent imaging systems such as synthetic aperture radar (SAR) have an inherent random phase, complex-valued nature. On the other hand sparse signal representation, which has mostly been exploited in real-valued problems, has many capabilities such as superresolution and feature enhancement for various reconstruction and recognition tasks. For complex-valued problems, the key challenge is how to choose the dictionary and the representation scheme for effective sparse representation. We propose a mathematical framework and an associated optimization algorithm for a sparse signal representation-based imaging method that can deal with these issues. Simulation results show that this method offers improved results compared to existing powerful imaging techniques.

**Index Terms:** sparse signal representation, complex-valued imaging, image reconstruction, coherent imaging, synthetic aperture radar.

## 1. INTRODUCTION

This paper presents a new image reconstruction technique based on sparse signal representation that can be used for complex-valued imaging systems. Many coherent imaging systems such as synthetic aperture radar (SAR), holography, magnetic resonance imaging, laser imaging, sonar imaging, and so on, have an inherent complex-valued nature [1]. Also, phase of the imaged field might be random and spatially uncorrelated in some applications such as SAR [2].

In these systems, straightforward application of image reconstruction techniques developed

originally for incoherent real-valued imaging systems will not produce high quality images. One of these techniques that have mostly been exploited in real-valued problems is sparse signal representation, which has many capabilities such as superresolution and feature enhancement for various reconstruction and recognition tasks.

Recent work on feature-enhanced complex-valued imaging [3] has ties to sparse representation. In particular, one interpretation of this technique involves sparse representation with some fixed, specific dictionaries. Our work generalizes that work to sparse representation with arbitrary overcomplete dictionaries.

The key challenge for exploiting sparse representation in complex-valued problems is how to choose the dictionary and the representation scheme for effective sparse representation.

In the next sections we present a mathematical framework that deals with these issues. As presented in Section 2, we have used a general linear observation model, and applied sparse representation on the magnitude of the complex-valued scattered field. This then turns the image reconstruction problem into a joint optimization problem over the magnitude and the phase of the underlying field reflectivities. We present an iterative algorithm to solve this joint optimization problem. In the end of Section 2, a discussion on dictionary selection is presented. In Section 3 our experimental results are presented to show the effectiveness of this new method.

## 2. SPARSE REPRESENTATION FOR COMPLEX-VALUED PROBLEMS

This section contains a description of our sparse representation technique for complex-valued problems. We start with describing our general

observation model. Next we present our sparse representation scheme and the related optimization problem. Then we present our algorithm to solve this optimization problem. Finally a discussion about proper dictionary selection is presented.

## 2.1 Observation model

We use the following general observation model:

$$y = T f + n \quad (1)$$

where  $y$  is the sampled measured data,  $f$  is the unknown scene or object reflectivity image, and  $n$  is noise; all are complex and column-reordered as vectors.  $T$  represents a complex-valued discrete observation kernel.  $T$  could be, for example, a band-limited Fourier transform operator matrix, or a projection operator matrix as in SAR or other tomographic imaging system [3,4].

## 2.2 Sparse representation scheme

In many applications of imaging systems introduced in Section 1, such as SAR, we could have a sparse representation in a proper domain for magnitude of complex scattered field (image). This means that we can write:

$$|f| = \Phi \alpha \quad (2)$$

Where  $\Phi$  is an appropriate dictionary for our application, and  $\alpha$  is the new domain coefficient vector with which the magnitude of scattered field can be sparsely represented.

We can write  $f = P |f|$ , where  $P = \text{diag}\{e^{j\phi_i}\}$ , and  $\phi_i$ 's are the unknown phases of each image vector element  $f_i$ . So we can rewrite our observation model as:

$$y = T f + n = T P |f| + n = T P \Phi \alpha + n \quad (3)$$

If we knew  $P$  (the unknown image vector elements phases), using a sparsity regularization method such as an extension of basis pursuit [5] as follows, we could find an estimate of  $\alpha$  and hence of the image itself:

$$\hat{\alpha} = \arg \min_{\alpha} \|y - T P \Phi \alpha\|_2^2 + \lambda \|\alpha\|_p^p \quad (4)$$

where  $\|\cdot\|_p$  denotes the  $\ell_p$ -norm and  $\lambda$  is a scalar parameter. However we don't know the image phases and hence  $P$ . We use the following approach to overcome this problem:

**a.** First we start with an initial estimate for  $f$  that could be a conventional reconstruction of  $f$ , so we can also produce an initial estimate of the image phase matrix  $P$ . In this way, we can solve the optimization problem in (4) and find a new estimate for  $\alpha$ .

**b.** Now we have a new estimate of  $\alpha$  and so  $|f|$ , and we should now find a new estimate for  $P$ . We can rewrite our observation model as:

$$y = T P |f| + n = T B \beta + n \quad (5)$$

where  $B = \text{diag}\{|f_i|\}$  and  $\beta$  is vector of unknown phases, hence a vector containing the diagonal elements of  $P$ . We can find an estimate of  $\beta$  as follows:

$$\hat{\beta} = \arg \min_{\beta} \|y - T B \beta\|_2^2 \quad \text{subject to } |\beta_i| = 1, \forall i \quad (6)$$

We replace the constrained optimization problem in (6), with the following unconstrained problem that incorporates a penalty term on the magnitudes of  $\beta_i$ 's:

$$\begin{aligned} \hat{\beta} &= \arg \min_{\beta} \|y - T B \beta\|_2^2 + \lambda' \sum_{i=1}^N (|\beta_i|^q - 1)^2 \\ &= \arg \min_{\beta} \|y - T B \beta\|_2^2 + \lambda' \|\beta\|_{2q}^{2q} - 2\lambda' \|\beta\|_q^q \end{aligned} \quad (7)$$

Solving this optimization problem will give us a new estimate for the phase vector  $\beta$  and so the matrix  $P = \text{diag}\{\beta\}$ .

c. We are now back to step (a) and we repeat the above steps until the algorithm converges to its final solution.

### 2.3 Solving the optimization problems

If we call the cost function of optimization problem (4)  $J(\alpha)$  and use the smooth approximation  $\|\alpha\|_p^p \approx \sum_{i=1}^M (|\alpha_i|^2 + \varepsilon)^{p/2}$ , where  $\varepsilon$  is a small positive constant, to avoid nondifferentiability problems of the  $\ell_p$ -norm around the origin, then the gradient of  $J(\alpha)$  will be:

$$\nabla J(\alpha) = H(\alpha) \alpha - 2(TP\Phi)^H y \quad (8)$$

where

$$H(\alpha) = 2(TP\Phi)^H(TP\Phi) + \lambda p \Lambda(\alpha)$$

$$\Lambda(\alpha) = \text{diag} \left\{ \frac{1}{(|\alpha_i|^2 + \varepsilon)^{1-p/2}} \right\} \quad (9)$$

Using the quasi-Newton iterative method developed in [3], which is well suited for this kind of nonquadratic optimization problems, with approximate Hessian  $H(\alpha)$ :

$$\hat{\alpha}^{(n+1)} = \hat{\alpha}^{(n)} - \gamma [H(\hat{\alpha}^{(n)})]^{-1} \nabla J(\hat{\alpha}^{(n)}) \quad (10)$$

And after substituting (8) in (10) and rearranging we obtain the iterative algorithm:

$$H(\hat{\alpha}^{(n)}) \hat{\alpha}^{(n+1)} = (1-\gamma) H(\hat{\alpha}^{(n)}) \hat{\alpha}^{(n)} + 2\gamma(TP\Phi)^H y \quad (11)$$

The algorithm can be started from an initial estimate of  $\alpha$  and run until convergence occurs. Solution of the optimization problem (7) can be derived in a similar manner:

$$H'(\hat{\beta}^{(n)}) \hat{\beta}^{(n+1)} = (1-\gamma) H'(\hat{\beta}^{(n)}) \hat{\beta}^{(n)} + 2\gamma(TB)^H y \quad (12)$$

where

$$H'(\beta) = 2(TB)^H(TB) + 2\lambda'q \Lambda_1(\beta) - 2\lambda'q \Lambda_2(\beta) \quad (13)$$

$$\Lambda_1(\beta) = \text{diag} \left\{ \frac{1}{(|\beta_i|^2 + \varepsilon)^{1-q}} \right\}$$

$$\Lambda_2(\beta) = \text{diag} \left\{ \frac{1}{(|\beta_i|^2 + \varepsilon)^{1-q/2}} \right\} \quad (14)$$

### 2.4 Dictionary selection

Selection of the proper dictionary  $\Phi$  is an important part of this method. This dictionary should sparsely represent the magnitude of the complex-valued image, and so it depends on the application and the type of objects or features of interest in our image.

#### 2.4.1 Overcomplete shape-based dictionaries

If our scene can be represented as combination of some limited simple shapes such as points, lines, squares, and so on, then an efficient dictionary can be constructed by gathering all possible positions of these fundamental elements in an overcomplete dictionary. The use of such an overcomplete dictionary is demonstrated in Section 3 on some synthetic scenes.

It is also possible to use more general, possibly multiresolution dictionaries that are well known for sparse representation of two dimensional signals (images). We present some possible choices below:

#### 2.4.2 Biorthogonal wavelet transforms

Previous works have established that wavelet transform can sparsely represent natural scene images [6,7]. The application of wavelet transforms to image compression leads to impressive results over Fourier-based representations such as the discrete cosine transform (DCT). However, wavelet transform offers only a fixed number of directional elements independent of scale.

#### 2.4.3 Curvelet Transform

Curvelet transform enables directional analysis of an image in different scales. This dictionary is well suited for enhancing features like edges and smooth curves in an image.

#### 2.4.4 Discrete cosine transform (DCT)

Both of above general dictionaries are suitable for piecewise smooth content images, however for sparse representation of periodic patterns, as in some textures, they may not be good choices and other dictionaries such as DCT may be preferred. DCT is known to be well suited for first order Markov stationary signals [6]. For nonstationary signals it could be applied in blocks.

There exist many other popular dictionaries, which we don't mention here for the sake of brevity. We should just point out that any such dictionary could be used in our framework, if it is appropriate for the particular application of interest.

### 3. EXPERIMENTAL RESULTS

We present here our results of experiments with various synthetic images to demonstrate different capabilities of this new method. In our experiments we have selected a spotlight-mode synthetic aperture radar (SAR) modality as our complex-valued sensing system. In all presented results we have used parameters of an X-band SAR of 10 GHz center frequency and 0.375 m range and azimuth resolution, except for results that show superresolution capability, in which resolution values are doubled so that system resolution is a multiple of image pixel size and we can put multiple scatterers in one resolution cell and observe the results. All images consist of  $32 \times 32$  complex-valued pixels. To be able to compare the results, we also present results of conventional reconstruction as well as nonquadratic regularization method [3] that have recently been developed for point and region enhanced SAR image reconstruction.

First we show an important capability of this method that is superresolution, which means that it can reconstruct image details under bandwidth limitations. To show this property, we apply our method to a synthetic scene composed of eight point scatterers with unit reflectivity magnitude and random (uniform) uncorrelated phase. We set our system parameters so that system resolution is two times of image pixel size, so we seek superresolution reconstructions. Fig. 1 (b) shows

conventional spotlight mode SAR reconstruction using polar format algorithm [8] that cannot resolve closely-spaced scatterers and suffers from high sidelobes.

Fig. 1(c) shows the result of nonquadratic regularization reconstruction method with penalties for both point and region feature enhancement. Note that this method also has superresolution capability when we just use point enhancement penalty, however in this case we allow the possibility of both point and region-based features in the scene, e.g. due to lack of more specific prior knowledge on the scene. As a result, this technique fails to reconstruct the scene accurately.

Fig. 1(d) shows the result of the sparse representation method we propose in this paper, with parameters  $p=0.7$ ,  $\lambda=3$ ,  $q=0.3$ , and  $\lambda'=0.07$ . We have used the conventional reconstruction as the initial estimate of  $f$ . The dictionary used here is the same as described in the next experiment.

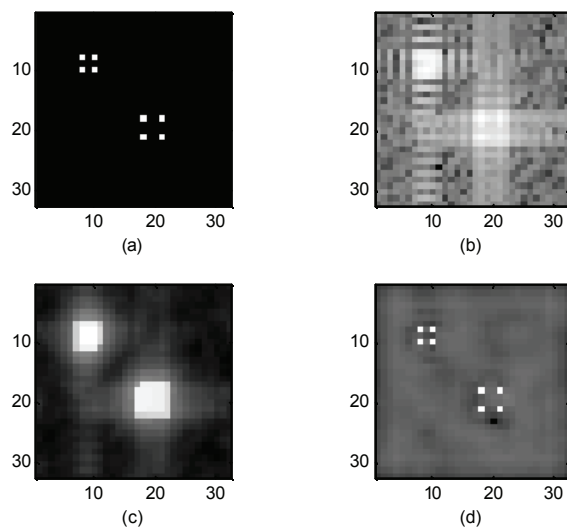


Fig. 1. Superresolving a scene with isolated point scatterers. (a) True scene (b) Conventional reconstruction (c) Point-region-enhanced nonquadratic regularization (d) Sparse representation-based reconstruction.

In order to demonstrate the capabilities of this new method and contrast it with existing methods, we now consider a more general scene composed

of both point targets and distributed targets, shown in Fig. 2(a). Parameters used in this result are  $p=0.9$ ,  $\lambda=3$ ,  $q=1$ , and  $\lambda'=0.2$ . Here we use an overcomplete shape-based dictionary. In particular our dictionary consists of

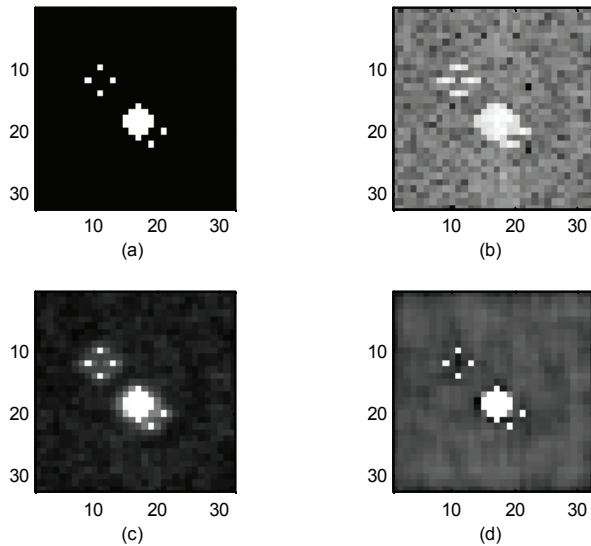


Fig. 2. Scene composed of point and distributed targets. (a) True scene (b) Conventional reconstruction (c) Point-region-enhanced nonquadratic regularization (d) Sparse representation-based reconstruction.

points as well as squares of various sizes at every possible location in the scene. We note that such a dictionary can be used to sparsely represent many interesting scenes. Superiority of sparse representation method over others can be clearly observed in this figure.

To be more realistic, in the next experiment we use a synthetic image, constructed from the MIT Lincoln Laboratory Advanced Detection Technology Sensor (ADTS) data set [9] by segmentation techniques, as shown in Fig. 3(a). In these type real scenes, we may not have enough prior information for using overcomplete shape-based dictionaries and/or we may need more general dictionaries that can sparsely represent many probable different scenes. Here we use the wavelet transform which is a multiresolution dictionary and can sparsely represent many natural scenes containing information at multiple

spatial scales. Parameters used in this experiment are  $p=0.6$ ,  $\lambda=17$ ,  $q=1$ , and  $\lambda'=10$ . We have used Haar wavelet as our dictionary in this result. Again we see near perfect reconstruction with our sparse signal representation-based method.

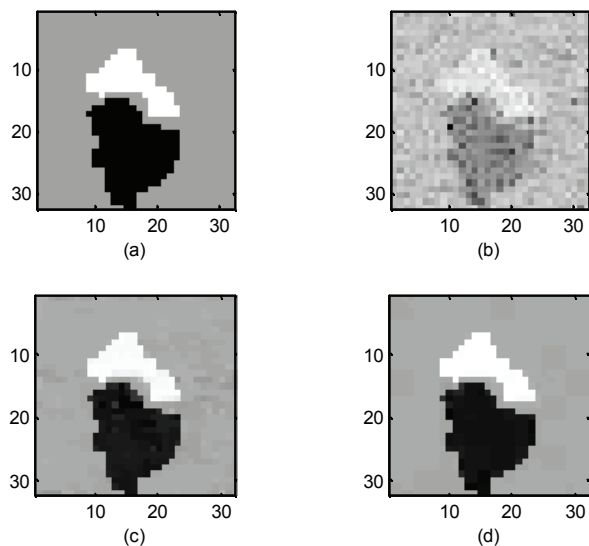


Fig. 3. Synthetic ADTS phantom image reconstruction (a) Synthetic scene (b) Conventional reconstruction (c) Point-region-enhanced nonquadratic regularization (d) Sparse representation-based reconstruction.

#### 4. CONCLUSIONS

In this paper we have presented a new method for complex-valued image reconstruction based on sparse signal representation, which brings many capabilities of sparse signal representation to the content of complex-valued imaging systems. We have developed a mathematical framework for this purpose and shown its effectiveness on various synthetic scenes.

#### REFERENCES:

- [1] M. Çetin, W. C. Karl, and A. S. Willsky, "Feature-preserving regularization method for complex-valued inverse problems with application to coherent imaging", *Optical Engineering*, 45(1) : 017003, January 2006.
- [2] D. C. Munson, Jr. and J. L. C. Sanz, "Image reconstruction from frequency-offset Fourier data," *Proc. IEEE*, vol. 72, pp. 661–669, June 1984.
- [3] M. Çetin and W.C. Karl, "Feature-enhanced synthetic aperture radar image formation based on

- nonquadratic regularization", *IEEE Trans. Image Processing*, vol. 10, pp. 623–631, April 2001.
- [4] D. C. Munson Jr., J. D. O'Brien, and W. K. Jenkins, "A tomographic formulation of spotlight-mode synthetic aperture radar", *Proceedings of the IEEE*, 71:917–925, August 1983.
- [5] S. S. Chen, D. L. Donoho, and M. A. Saunders, "Atomic decomposition by basis pursuit", *SIAM J. Sci. Comput.*, Vol. 20, pp. 33-61, August 1998.
- [6] J. L. Starck, M. Elad, and D. L. Donoho, "Image decomposition via the combination of sparse representations and a variational Approach", *IEEE Trans. Image Processing*, Vol. 14, pp. 1570-1582, October 2005.
- [7] D. L. Donoho and I. Johnstone, "Ideal spatial adaptation via wavelet shrinkage", *Biometrika*, vol. 81, pp. 425-455, 1994.
- [8] W. G. Carrara, R. S. Goodman, and R. M. Majewski, *Spotlight Synthetic Aperture Radar: Signal Processing Algorithms*. Boston, MA: Artech House, 1995.
- [9] Air Force Research Laboratory, Model Based Vision Laboratory, Sensor Data Management System ADTS. [Online] available: <http://www.mbvlab.wpafb.af.mil/public/sdms/datasets/adts/>.